



**HAL**  
open science

# Rayleigh Surface Acoustic Wave As an Efficient Heating System for Biological Reactions: Investigation of Microdroplet Temperature Uniformity

Thibaut Roux-Marchand, Denis Beyssen, Frederic Sarry, Omar Elmazria

► **To cite this version:**

Thibaut Roux-Marchand, Denis Beyssen, Frederic Sarry, Omar Elmazria. Rayleigh Surface Acoustic Wave As an Efficient Heating System for Biological Reactions: Investigation of Microdroplet Temperature Uniformity. IEEE Transactions on Ultrasonics, Ferroelectrics and Frequency Control, 2015, 62 (4), pp.729-735. 10.1109/TUFFC.2014.006710 . hal-01293132

**HAL Id: hal-01293132**

**<https://hal.science/hal-01293132>**

Submitted on 18 Apr 2020

**HAL** is a multi-disciplinary open access archive for the deposit and dissemination of scientific research documents, whether they are published or not. The documents may come from teaching and research institutions in France or abroad, or from public or private research centers.

L'archive ouverte pluridisciplinaire **HAL**, est destinée au dépôt et à la diffusion de documents scientifiques de niveau recherche, publiés ou non, émanant des établissements d'enseignement et de recherche français ou étrangers, des laboratoires publics ou privés.

# Rayleigh surface acoustic wave as an efficient heating system for biological reactions: Investigation of microdroplets temperature uniformity

T. Roux-marchand, D. Beyssen, F. Sarry, and O. Elmazria, *Member, IEEE*

**Abstract**—When a microdroplet is put on the Rayleigh Surface Acoustic Wave path, longitudinal waves are radiated into the liquid and induce several phenomena such as the well-known surface acoustic wave streaming. At the same time, the temperature of microdroplet increases as it has been shown. In this paper, we study the temperature uniformity of microdroplet heated by Rayleigh Surface Acoustic Wave for discrete microfluidic applications such as biological reactions. To precisely ascertain the temperature uniformity and not interfere with the biological reaction, we use an infrared camera. We then have tested the temperature uniformity as a function of three parameters: the microdroplet volume, the Rayleigh surface acoustic wave frequency and the continuous applied radio frequency power. Based on these results, we propose a new device structure to develop a future lab on a chip based on temperature's reactions.

**Index Terms** — Microfluidic, SAW streaming, microdroplet heating, biological reaction.

## I. INTRODUCTION

SURFACE acoustic wave (SAW) devices are widely employed in telecommunication systems as filters, delay lines or resonators. If these applications constitute the first and the main market for the SAW devices, their use in sensor and actuator applications, such as chemical and biochemical sensors, was also developed in the few last decades [1]. Recently, the microfluidic research community has expressed particular interest in the use of SAW devices for many reasons. Their fabrication technology is relatively cost-effective, they are based on simple electrodes network and due to their small size, they should be added into microscale system promising an excellent solution for fluid miniaturization platforms. They should be used as a digital microfluidic technology as it has been shown [2-4]. Compared with continuous-flow microfluidic, SAW devices do not require microvalve and micropump which can be expensive,

difficult to achieve and size consuming [5]. The reduction of device scales allows the decrease of reaction time and cost reagents, enhance efficiency and sensitivity of the analysis [6,7] and are the main interest to develop micro-Total Analysis Systems ( $\mu$ TAS).

Rayleigh Surface Acoustic Wave (R-SAW), which presents an elliptical displacement, becomes a leaky-SAW when they encounter droplet loaded on the wave path. Longitudinal wave are then radiated into the liquid. This induces, according to the wave's power, an internal streaming, the vibration of the liquid free-surface, droplet's heating, motion of droplet and atomization.

Currently, the heating process with industrial thermocyclers suffers from slow heating (max. 3.3°C/sec for Techne Thermocycler) and cooling to perform thermal reaction. Miniaturized systems address some of these concerns due to their reduced mass and volume. There are many heating technics for microfluidic system. Until today, localized heating designs are mainly by Peltier heaters, resistive heaters and, more rarely, by other technics as transistors heaters, microwave or optical heating [8-16]. However, the heating is localized at a fixed location. Thus, the microdroplets need to put directly on the heater system. With R-SAW device, the droplets are not put on the transducer. They can be heated anywhere on the piezoelectric substrate on the wave's path. More, compared to others systems, the interaction between surface acoustic wave and microdroplet induces internal streaming which allows heat transfer by forced convection in liquid at the same time than heating. This improves the temperature stabilization time and therefore allows to reach thermodynamic equilibrium faster than a static sample where conduction mechanism is predominant. In addition, it is possible to mix, to heat, to move and to atomize the droplet put on the SAW path just by varying the power applied to the transducer. This makes it a good choice to interact with microdroplet in order to develop lab on chip applications. The heating by surface acoustic wave can reach high temperature (more than 100°C) as shown in other studies [17,18] and can be used to catalyze some thermal biological and chemical reactions, including the polymerase chain reaction, hybridization. However, current studies do not focus on the uniformity of the microdroplet temperature, which is very

Manuscript received December \*\*, 2013; accepted \*\*\*\* \*\*, 2014. This work was supported in part by the French ANR (ANR-12-BS09-021).

T. Roux-Marchand, D. Beyssen, F. Sarry and O. Elmazria are with the Institut Jean Lamour, UMR 7198 CNRS-Université de Lorraine, Faculté des Sciences et Technologies, BP 70239 F-54506 VANDOEUVRE les NANCY cedex (e-mail: thiabaut.roux-marchand@univ-lorraine.fr).

important for lots of biological and chemical reactions.

Hence the study of the temperature uniformity of the microdroplet has been investigated to precisely ascertain the microdroplet temperature. There are different techniques available for temperature measurements [18-20], contact as well as non-contact methods. For R-SAW devices, only non-intrusive methods like infrared thermography may be used so as to not interfere with the thermal system. Our approach is to record the temperature of a microdroplet heated by R-SAW with an infrared camera. The emissivity of each solution has been determined before using thermalized structure, a black body, the solution (water-glycerin mixture) and the infrared camera.

In this paper, the microdroplet temperature uniformity, expressed by the temperature standard deviation, is studied as a function of the applied power to Interdigital Transducers (IDT). The effect of the wavelength of SAW on the temperature uniformity is also studied as well as the microdroplets volume. We discussed the heating uniformity by monitoring the liquid temperature under different experimental conditions. Finally, we propose a new device to enhance the temperature uniformity.

## II. EXPERIMENTAL

### A. SAW Device

R-SAWs are generated by IDT realized with sputtered aluminum and conventional photolithography on a piezoelectric 128°Y-X cut lithium niobate ( $\text{LiNbO}_3$ ) substrate. It was chosen because it is a single crystal, which induces low propagation losses, and presents an electromechanical coupling coefficient of 5.5% [21].

A typical bidirectional SAW transducer is sketched in Fig. 1. SAW wavelength is determined by the transducer pitch  $\lambda$  as shown in Fig. 1. The resonant frequency  $f_0$  (Hz) of R-SAW device is calculated by (1) where  $v$  ( $\text{m}\cdot\text{s}^{-1}$ ) is the phase velocity

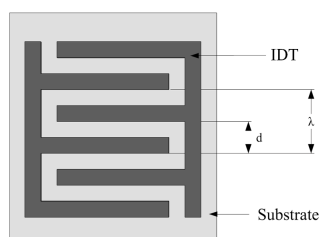


Fig. 1. Typical bidirectional transducer

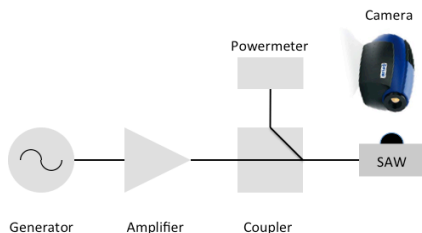


Fig. 2. Experimental setup for self-heating measurements

of R-SAW in the substrate:

$$f_0 = \frac{v}{\lambda} \quad (1)$$

### B. Experimental set-up

The schematic in Fig. 2. illustrates the experimental setup used for heating measurements. An RF signal generator (Hewlett Packard HP8648C) is connected to the power amplifier (Minicircuits ZHL-5W-1) which feeds the SAW device via a directional coupler (MinicircuitsZFDC-20-1H). A powermeter (Agilent Technologies E4417A) measures the applied electrical power  $P_{\text{IDT}}$  to the IDT. The microdroplet is placed on acoustic path at 10mm from IDT. An infrared camera (FLIR SC5600) is positioned above the sample with a temperature resolution lower than 30mK, spatial resolution of 5  $\mu\text{m}$ , a recording speed of 100 images per second and a spectral response between 2.5 and 5.1 $\mu\text{m}$ . Dedicated software from FLIR leads to drive the infrared camera and collect data. The camera is thus used to follow the heat of the droplets deposited on the elastic path in both scales: spatial and temporal.

### C. Microdroplet temperature

The temperature of a 10 $\mu\text{l}$  glycerol microdroplet is shown on Fig. 3. as a function of time with three power applied to the IDT and for 200 $\mu\text{m}$  SAW wavelength. The temperature is

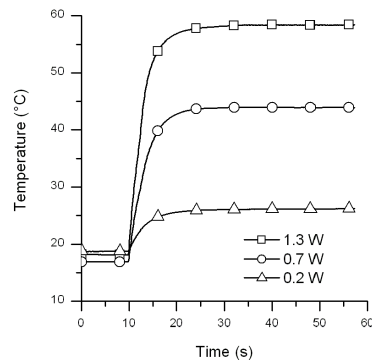


Fig. 3. Temperature of 10 $\mu\text{l}$  glycerol microdroplet as function of time and for several applied power to the IDT (1.3W, 0.7W, and 0.2W). The SAW wavelength is 200 $\mu\text{m}$ .

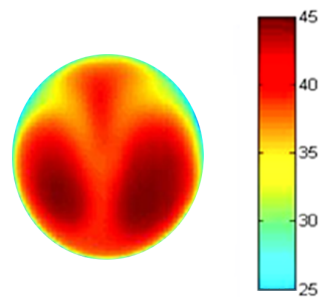


Fig. 4. Example of an infrared image of a 10 $\mu\text{L}$  microdroplet on the R-SAW path. The applied power, the wavelength, and the dynamic viscosity are respectively 1W, 200 $\mu\text{m}$  and 10.8mPa.s. The image is taken after 30s of irradiation when the mean temperature remains constant. One can clearly observe the non-uniformity of the droplet temperature.

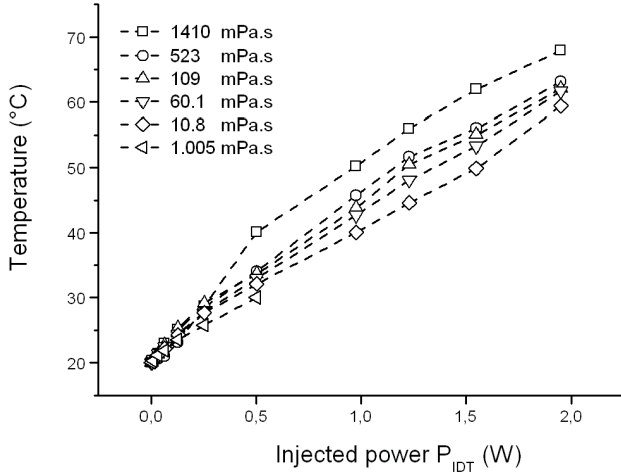


Fig. 5. Temperature of 10µL microdroplet as function of applied power to the IDT and for several liquid viscosities (water-glycerin mixture). The dynamic viscosities are given at 20°C. The R-SAW wavelength is 200µm and the volume is 10µL.

given by the software of the infrared camera and is the mean of all pixels of the microdroplet infrared image (see Fig. 4.). As we can see on Fig. 3., the power is put on after 10s and the temperature is stabilized after 30s of irradiation. The temperature increases with applied power and the time constant is about 5s. For all following measurements, the temperature and the standard deviation are noted after 30s of SAW irradiation, when the temperature has reached the steady state.

The temperature of a microdroplet is shown on Fig. 5. as a function of applied power to the IDT and the dynamic viscosity. Water-Glycerin mixture has been used in order to explore a wide range of dynamic viscosity, from 1.005mPa.s to 1410 mPa.s (20°C). As expected and in conformity with previous work [17,18,22], the microdroplet temperature heated by R-SAW increases with applied power and with dynamic viscosity. Infrared image of microdroplet will be very useful to obtain information on the temperature uniformity.

Liquid droplet heating effect depends on the attenuation of the longitudinal wave in the droplet. The attenuation of the longitudinal wave is given by the next relation [23] :

$$\alpha = \frac{R}{2} \frac{\omega^2}{c_L^3} \quad (2)$$

with

$$R = \frac{1}{\rho_L} \left( \frac{4}{3} \mu + \mu' + \frac{K}{C_p} (\gamma - 1) \right) \quad (3)$$

where  $\omega$  is the pulsation,  $c_L$  the velocity of wave in the liquid,  $\rho_L$  the density of liquid,  $\mu$  the dynamic viscosity,  $\mu'$  the volume viscosity,  $K$  the thermal conductivity of liquid,  $C_p$  the heat capacity at constant pressure, and  $\gamma$  the ratio  $C_p/C_v$  with  $C_v$  the heat capacity at constant volume. With next calculations, we neglect the last term because the ratio  $K/C_p$  will be low and close to zero. For water and glycerin, the volume viscosity is well known. For water,  $\mu' = 2.8\mu$  [23],  $K=0.6W.m^{-1}.K^{-1}$ ,  $C_p = 4182J.Kg^{-1}.K^{-1}$ , the attenuation  $\alpha$  with a

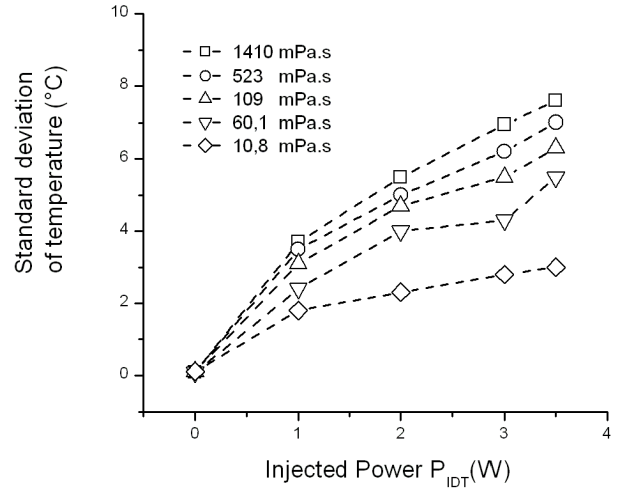


Fig. 6. Microdroplet temperature uniformity, reflected by its temperature standard deviation, as a function of power applied to the IDT for different liquid viscosity. The liquid is a 10µL microdroplet and the R-SAW wavelength is 100µm.

200µm wavelength is  $8.6m^{-1}$  which indicates that 95% of the longitudinal wave energy is dissipated in water after a distance of 34.8cm ( $3\alpha^{-1}$ ). For glycerin, the attenuation  $\alpha$  is  $2372m^{-1}$  which indicates that 95% of the longitudinal wave energy is dissipated in glycerin after a distance of 1.2mm ( $3\alpha^{-1}$ ). The attenuation for all considered liquid is between  $8.6m^{-1}$  and  $2372 m^{-1}$  with 200µm SAW wavelength. By decreasing wavelength, and so increasing frequency (see eq. (1)), the attenuation increases. With lower wavelength 100, 50 and 25µm used in this study, the attenuation for all considered liquid is respectively between  $34.52m^{-1}$  and  $9488m^{-1}$ ,  $138.08m^{-1}$  and  $37952m^{-1}$ ,  $552.32m^{-1}$  and  $75904m^{-1}$ .

Concerning the heat dissipation of the microdroplet, the mainly heat transfer is by conduction into the substrate. The conduction through the atmosphere can be neglected because the air heat conductivity is low ( $0.027W.m^{-1}.K^{-1}$ ) whereas the one of the lithium niobate substrate is higher ( $5.6W.m^{-1}.K^{-1}$ ).

#### D. Infrared image

An example of an obtained infrared image from the camera is presented in Fig. 4. A 10µL microdroplet is positioned on the wave's path and R-SAW irradiated it. Energy dissipation by viscous friction leads to heat the liquid and an internal flow takes place. We see that the maximum's temperatures into the microdroplet are located where the two vortices are generated. Otherwise, we clearly note that the temperature is not uniform. To quantify these phenomena, we get the standard deviation of the temperature with all droplet pixels, which is given by the camera software. The uniformity is better with a low standard deviation.

### III. RESULTS AND DISCUSSION

#### A. Power effect

When increasing the power applied to IDT, the amplitude of R-SAW grows and the microdroplet average temperature is also enhanced as shown on Fig.5. In terms of liquid viscosity and power, it is possible to heat the microdroplet over 100°C [17,18,22] which is sufficient for several chemical and

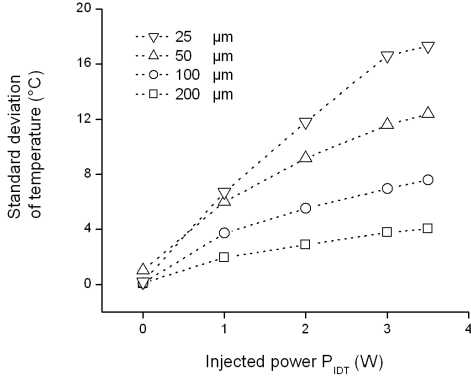


Fig. 7. Microdroplet temperature uniformity, reflected by the standard deviation of microdroplet temperature, as a function of power applied to the IDT for different R-SAW wavelength. The liquid is a 5  $\mu$ L glycerol microdroplet put on the SAW path.

biological reaction. For such temperature a lid will be added to limit evaporation. However, the standard deviation of microdroplet temperature also increases with power as shown on Fig. 6. Moreover, with a fixed power, the standard deviation grows with dynamic viscosity. This induces that the uniformity of microdroplet temperature degrades with the liquid viscosity and the applied power, i.e. when the microdroplet temperature increases. To reduce this effect, we study the effect of R-SAW wavelength and the microdroplet volume.

### B. R-SAW wavelength effect

We study the effect of R-SAW wavelength of our device. From equation (1), by changing the wavelength  $\lambda$  of the IDT from 200  $\mu$ m to 25  $\mu$ m, the frequency is adjusted from 20MHz to 160MHz. We irradiated the glycerol microdroplet with this new frequency signal. We note that a best uniformity is achieved with the longer R-SAW wavelength as shown on Fig. 7. At 25  $\mu$ m and 3.6W, the standard deviation of microdroplet temperature is above 16°C, while with the 200  $\mu$ m wavelength, it did not exceed 4°C. This is due to the attenuation of R-SAW at the liquid/solid interface which is given by the next equation [24]:

$$\alpha = \frac{1}{\lambda} \frac{\rho_l c_l}{\rho_s c_s} \quad (4)$$

where  $\alpha$  in  $m^{-1}$ ,  $\rho_l$  and  $c_l$  the density and the SAW velocity on the liquid respectively and  $\rho_s$  and  $c_s$  the density and the SAW velocity on the substrate respectively. We can see that the attenuation  $\alpha$  is inversely proportional to the wavelength. A longer R-SAW wavelength, leading to a low frequency (eq. (1)), induces a lower attenuation. In this way, the R-SAW propagates deeper at the liquid/solid interface. Figure 8 evidences this behaviors. For the smallest wavelengths, 200  $\mu$ m and 100  $\mu$ m, the R-SAW propagates deeper at the liquid/solid interface whereas with small wavelength, 50 and 25  $\mu$ m, the R-SAW is rapidly attenuated.

This induces different heat transfer mechanisms [25]. With longer wavelengths (200 and 100  $\mu$ m), the heat transfer is principally due to forced convection on all the volume of

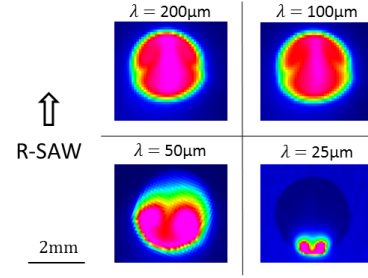


Fig. 8. Microdroplet heating with several wavelengths: 200, 100, 50 and 25  $\mu$ m. The liquid is a 10  $\mu$ L glycerol microdroplet put on the SAW path and the applied power to the IDT is 1.5W. The images are taken after 30s of irradiation. The acoustic aperture is greater than the size of the droplet, excepted for the device with 25  $\mu$ m wavelength where the acoustic aperture is 1mm.

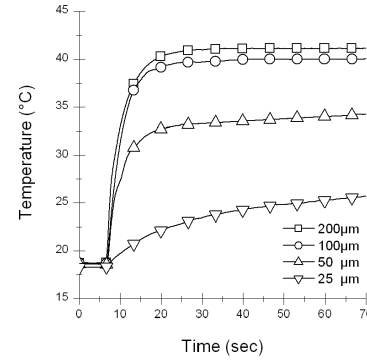


Fig. 9. Microdroplet temperatures as a function of time for four wavelengths (200, 100, 50 and 25  $\mu$ m) with a fixed applied power (0.5W). Liquid is glycerol and volume is 10  $\mu$ L. Power is put on after seven seconds.

microdroplet as shown on Fig. 8. After 30s of exposure, the thermodynamic equilibrium is reached. Indeed, the microdroplet temperature is stabilized, as shown on Fig. 9. and the standard deviation is the lower as presented on Fig. 7. In the case of small wavelengths (50 and 25  $\mu$ m), the conduction and forced convection mechanisms coexist. The attenuation being higher, the recirculation is then very close to the impact of R-SAW with the microdroplet, limiting thus that the convection occurs at all droplet volume (Fig. 8). This induces that, after 30s of irradiation, the thermodynamic state is still transient. Effectively, the Fig. 9. shows that the temperature of microdroplets heated by R-SAW with 25 and 50  $\mu$ m of wavelengths increases continuously with time. The temperature is still not stabilized and the standard deviation is higher. The heat transfer mechanism affects directly the time to achieve thermodynamic equilibrium, transfers by forced convection being faster than those by conduction [25]. For this microdroplet volume (10  $\mu$ l), it is important to work with low frequency to achieve thermodynamic equilibrium rapidly and to have the better temperature uniformity.

### C. Volume effect

As a function of the R-SAW wavelength, the volume of the microdroplet can play an important role. In the case of long wavelength (200  $\mu$ m, 20MHz), we report the effect of the

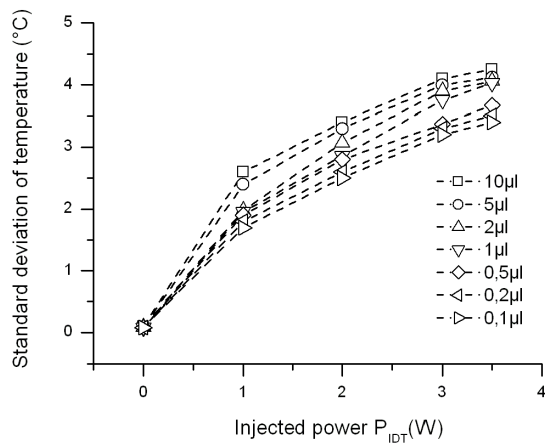


Fig. 10. Microdroplet temperature uniformity, reflected by the standard deviation of microdroplet temperature, as a function of power applied to the IDT with several microdroplet volume. The wavelength is  $200\mu\text{m}$  and the liquid is glycerol. The acoustic aperture is  $5\text{mm}$  and greater than the size of droplets. The measures are done after 30s of irradiation.

microdroplet volume on Fig. 10. As we can see, whatever the applied power to the IDT, the standard deviation of temperature increases with microdroplet volume. The microdroplet volume plays a less important role than the applied power and R-SAW wavelength as we saw before. Indeed, with a fixed power, the variation of the temperature standard deviation is low whatever microdroplet volume. The maximum variation of the standard deviation is observed for an applied power of  $3\text{W}$ . For that power and with a variation of the microdroplet volume of two decades, the variation of the temperature standard deviation did not exceed  $1^\circ\text{C}$ .

Figure 7 and Fig. 8 show that by reducing the wavelength, thus increasing the frequency, the length of the beam is reduced. Dentry et al. [26] has shown that the acoustic streaming jet produced by a SAW radiating into a fluid is dependent on the frequency. As the attenuation length scale of the acoustic wave decreases as  $1/\omega^2$ , the acoustic beam length into the fluid is reduced too and the power density in the jet is increased. Moreover higher frequencies drive recirculation effects within a smaller region closer to the source. As it is mentioned in [25,26], increasing the applied power will increase the streaming velocity although the flow structure of the jet appeared to remain relatively constant. Although our experimental conditions (smaller dimensions, glycerol liquid) are different, we still are under a laminar regime and we observed such effects.

Indeed, on Fig. 11., we report the standard deviation of temperature as a function of power and microdroplet volume for a  $25\mu\text{m}$  wavelength. Here, the volume plays an important role. With the lowest volume and a short wavelength of  $25\mu\text{m}$ , the heat transfer is mainly governed by forced convection because the frequency is in good agreement with the dimension of the droplet. The thermodynamic equilibrium is reached after 30s of irradiation and the standard deviation is then low. With higher volume, the thermodynamic state is transient and the standard deviation of temperature is strong. With the higher applied power ( $3.5\text{W}$ ), the standard deviation vary from  $5.1^\circ\text{C}$  ( $0.1\mu\text{l}$ ) to  $20.4^\circ\text{C}$  ( $10\mu\text{l}$ ) as the recirculation is closer to the source. So here, we can observe

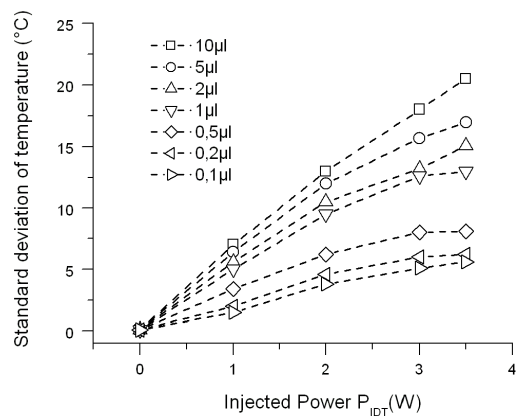


Fig. 11. Microdroplet temperature uniformity, reflected by the standard deviation of microdroplet temperature, as a function of power applied to the IDT with several microdroplet volume. The wavelength is  $25\mu\text{m}$ , the liquid is glycerol and the aperture is  $1\text{mm}$ . The measures are done after 30s of irradiation.

that with short wavelength, the temperature uniformity is improved using low volume.

#### IV. V.CONCLUSION

In this paper, we have studied the temperature uniformity of microdroplet heated by Rayleigh surface acoustic wave in view of microfluidic application as biological and chemical reaction. It has been shown that the applied power, the surface acoustic wave wavelength and the microdroplet volume influence the heating uniformity of the microdroplet. In order to obtain the best temperature uniformity, the surface acoustic wave wavelength and the microdroplet volume have to be chosen as a function of the final application. The microdroplet volume has an important impact on the temperature uniformity with short R-SAW wavelength. As we saw, the best uniformity is obtained with low microdroplet volume. Higher power causes increased jet momentum with a higher streaming velocity. The complex profile of the jet itself may explain why higher power is causing a larger standard deviation. Because some relative high temperature applications such as PCR reaction requires high applied power, it should be interesting to use a second IDT on the other side of the microdroplet and to consider a new design for IDTs. The two IDTs could than heat the microdroplet inducing a better temperature uniformity.

#### ACKNOWLEDGMENT

The authors would like to thank the ANR for their financial support (ANR-12-BS09-021).

#### REFERENCES

- [1] I. Voiculescu, A. Nordin, "Acoustic wave based MEMS devices for biosensing applications", *Biosensors and Bioelectronics*, vol. 33, pp. 1–9, 2012
- [2] D. Mark, S. Haeberle, G. Roth, F. Stettin and R. Zengerle, "Microfluidic lab-on-a-chip platforms: requirements, characteristics and applications", *Chem. Soc. Rev.*, vol. 39, pp. 1153-1182, 2010.

- [3] L. Y. Yeo and J.R. Friend, "Ultrafast microfluidics using surface acoustic waves", *Biomicrofluidics*, vol. 3, 012002, 2009.
- [4] T. D. Luong and N. T. Nguyen, "Surface Acoustic Wave Driven Microfluidics – A Review", *Micro and Nanosystems*, vol. 2, 2010.
- [5] R.B. Fair, "Digital microfluidics: is a true lab-on-a-chip possible?" *Microfluid Nanofluid*, 3, pp. 245–281, 2007.
- [6] S. Haeberlea, R. Zengerleab, "Microfluidic platforms for lab-on-a-chip applications", *Lab Chip*, 7, pp. 1094–1110, 2007.
- [7] D.R. Reyes, D. Iossifidis, P.A. Auroux, A. Manz, "Micro Total Analysis Systems. 1. Introduction, Theory, and Technology", *Anal. Chem*, 74, pp. 2623–2636, 2002.
- [8] G. Maltezos, M. Johnston, A. Scherer, "Thermal management in microfluidics using micro-Peltier junctions", *Appl Phys Lett*, vol. 87(15), pp.1–3, 2005
- [9] I. Park, Z. Li, A.P. Pisano, R.S. Williams, "Selective surface functionalization of silicon nanowires via nanoscale joule heating", *Nano Lett*, vol. 7(10), pp.3106–3111., 2007
- [10] C.Y. Lee, G.B. Lee, J.L. Lin, F.G. Huang, C.S. Liao, "Integrated microfluidic systems for cell lysis, mixing/pumping and DNA amplification", *J Micromech Microeng*, vol. 15(6), pp. 215–223, 2005
- [11] BC. Giordano, J. Ferrance, S. Swedberg, A.F.R. Hühmer, J.P. Landers, "Polymerase chain reaction in polymeric microchips: DNA amplification in less than 240 seconds", *Anal Biochem*, vol. 291(1), pp. 124–132, 2001
- [12] J.J. Shah, S.G. Sundaresan, J. Geist, D.R. Reyes, J.C. Boots, M.V. Rao, M. Gaitan, "Microwave dielectric heating of fluids in an integrated microfluidic device", *J Micromech Microeng*, vol.17 (11), pp. 2224–2230, 2007
- [13] M. Graf, U. Frey, S. Taschini, A. Hierlemann, "Micro hot plate-based sensor array system for the detection of environmentally relevant gases", *Anal Chem*, vol. 78(19), pp. 6801–6808, 2006.
- [14] D. Issadore, K.J. Humphry, K.A. Brown, L. Sandberg, D.A. Weitz, R.M. Westervelt, "Microwave dielectric heating of drops in microfluidic devices", *Lab Chip*, vol. 9(12), pp.1701–1706, 2009
- [15] H. Kim, S. Vishniakou, G.W. Farris, "Petri dish PCR: Laser-heated reactions in nanoliter droplet arrays", *Lab Chip*, vol. 9(9), pp.1230–1235., 2009
- [16] H. Terazono, A. Hattori, H. Takei, K. Takeda, K. Yasuda, "Development of 1480 nm photothermal high-speed real-time polymerase chain reaction system for rapid nucleotide recognition", *Jpn J Appl Phys*, vol. 47, pp. 5212–5216, 2008
- [17] T.Roux-Marchand, D.Beyssen, F. Sarry, S. Grandemange, O. Elmazria, "Rayleigh Surface Acoustic Wave compatibility with microdroplet polymerase chain reaction", *Int. J. Microscale Nanoscale Thermal Fluid Transport Phenomena*, vol. 4, pp. 231–248, 2013
- [18] J. Kondoh, N. Shimizu, Y. Matsui, M. Sugimoto, S. Shiokawa, "Development of temperature-control system for liquid droplet using surface acoustic wave devices", *Sensors and Actuators A*, 149, pp. 292–297, 2009.
- [19] S. Ito, M. Sugimoto, Y. Matsui, J. Kondoh, "Study of surface acoustic wave streaming phenomenon based on temperature measurement and observation of streaming in liquids", *Japanese Journal of Applied Physics*, vol. 46, no 7B, pp. 4718–4722, 2007.
- [20] J. El-Ali, I.R. Perch-Nielsen, C.R. Poulsen, D.D. Bang, P. Telleman, A. Wolff, "Simulation and experimental validation of SU-8 based PCR thermocycler chip with integrated heaters and temperature sensor", *Sensors and Actuators A*, 110, pp. 3–10, 2004.
- [21] K. Shibayama, Y. Yamanouchi, H. Sato, T. Meguro, "Optimum cut for rotated Y-cut LiNbO<sub>3</sub> crystal used as the substrate of acoustic wave filters", *Proc. IEEE*, 64, no. 5, pp. 595–597, 1973.
- [22] T. Roux-Marchand, D. Beyssen, F. Sarry, S. Grandemange, O. Elmazria "Microfluidic heater assisted by Rayleigh Surface Acoustic Wave on AlN/128°Y-X LiNbO<sub>3</sub> multilayer structure", *IEEE International Ultrasonics Symposium (IUS)*, pp.1706, 2012.
- [23] T. Litovitz, C. Davis, "Structural and shear relaxation in liquids", *Physical acoustics*, 2A, 1965
- [24] R. M. Arzt, E. Salzmann, K. Dransfeld, "Elastic surface waves in quartz at 316 mhz", *Applied Physics Letters* 10, 165 (1967); doi: 10.1063/1.1754894
- [25] D. Beyssen, T. Roux-Marchand, I. Perry and F.Sarry, "Correlation of rayleigh-saw streaming and thermal effect for prediction of heat transfer mechanism(s) within microdroplet", *The 17th International Conference on Miniaturized Systems for Chemistry and Life Sciences*, 2013, in press.
- [26] M.B. Dentry, L.Y. Yeo, J.M. Friend, "Frequency effects of the scale and behavior of acoustic streaming", *Physical Review E* 89, 013203 (2014).



Thibaut Roux-Marchand was born in 1988 in Nancy, France. He received his M.S. degree in embedded systems and microsystems in 2010 and the Ph.D degree in physics in 2013 from Lorraine University, France. Presently, he is a teaching assistant in IUT Nancy-Brabois, Lorraine University. These research works concern microfluidic systems assisted by surface acoustic waves at the Institut Jean Lamour, Lorraine University and CNRS, France. His principal research concerns the heating of microdroplet by Rayleigh surface acoustic wave in view of biological and chemical reactions.



Denis Beyssen was born in 1979 in Brive-la-Gaillarde, France. He received the Master degree in Physics and Chemistry (2003) from the University of Limoges and the Ph.D. degree in Microsystem (2006) from the University of Nancy, France. He joined the Institut Jean Lamour (IJL) of University de Lorraine as Associate Professor in 2007. His current interests concern the study of R-SAW/Liquid interaction for biocomponents's realization.



Frederic Sarry received the M.S. degree in Optoelectronic (1995) and the Ph.D. degree in Electronic (1998) from the University of Metz, France. He joined the University de Lorraine as Associate Professor in 1999 and became a full Professor in 2013. In 1999, he joined the Institut Jean Lamour, Nancy, France, as a permanent staff member. He has been the head of the Electrical Engineering Department at Nancy Technological Institute and he has recently joined as invited Professor the laboratory of Biophotonic of Sherbrooke University (Canada) with Pr. Paul Charette. He is now with ESSTIN (French Engineering School) and assistant director of the department "Nanomateriaux, Électronique et Vivant" at IJL. He works on piezoelectric films (ZnO, AlN) for surface acoustic wave (SAW) sensors (pressure, gas, temperature). His current interests are biocomponents assisted by SAW.



Omar Elmazria was born in Casablanca in 1968. He received the M.S. degree in industrial computer science and optoelectronic conjointly from the Universities of Metz, Nancy I, France, and the National Polytechnic Institute of Lorraine, France, in 1993, and the Ph.D. degree in electronics from Metz University, France, in 1996. In 1997, he joined the University of Nancy I as Associate Professor of electronic and communication systems and as Professor in 2003. Was the Head of the Micro and Nanosystems Group within the Institut Jean Lamour, Nancy, France. His research includes thin films for microelectromechanical-systems applications, surface-acoustic-wave devices for sensing applications, and high-frequency filters resonators based on layered structures, including diamond, AlN, and ZnO; microfluidic systems; wireless sensors, etc. He is the author of more than 120 papers in refereed international journals and in proceeding of international conferences. Prof. Elmazria is a member of IEEE Society from 2001, a member of the Technical Program Committee of the IEEE International Ultrasonics Symposium, Co-Chairman and member of the scientific committee of the IEEE International Conference on Electronic and Measurement Instrumentation (ICEMI), and a member of the Institut Universitaire de France (IUF).